LA-UR-22-30182

Approved for public release; distribution is unlimited.

Title:	An Investigation of Variables Affecting Plutonium Hydriding (20210946DI): Surface Phase Transitions and Reactions
Author(s):	Newman, Christopher Kyle
Intended for:	Report
Issued:	2022-09-30

An Investigation of Variables Affecting Plutonium Hydriding (20210946DI): Surface Phase Transitions and Reactions, C. Newman

1. Introduction

1.1 Tusas. Tusas [20, 18, 62, 61, 45], developed at LANL, is a general, flexible code for solving coupled systems of nonlinear partial differential equations (PDEs). Tusas was originally developed for phase field simulation of solidification (see [33, 6, 32]) and evolution of polycrystalline solid mechanics (see [16]). Tusas is particularly developed for PDEs compatible with structured or unstructured Lagrange (nodal) finite element discretizations and explicit (Euler) or implicit (Euler, Trapezoid, BDF2) temporal discretizations.

The Tusas approach consists of a finite element spatial discretization of the fully-coupled nonlinear system, which is treated explicitly or implicitly in time with a preconditioned Jacobian-free Newton-Krylov (JFNK) method. As the JFNK method only requires a residual, from an implementation standpoint, Tusas allows a flexible framework as it only requires the user to implement code for the residual equation. The key to efficient implementation of JFNK is effective preconditioning. As the dominant cost of JFNK is the linear solver, effective preconditioning reduces the number of linear solver iterations per Newton iteration. The preconditioning strategy in Tusas is based on block factorization and algebraic multigrid that allows an efficient, implicit time integration. As such, Tusas allows flexible preconditioning as it only requires the user to implement code for a row of the preconditioning matrix. In addition, configuration of the nonlinear system and preconditioner can be performed at runtime.

Most simulation e ort prior to this work has been focused on microstructure evolution of dilute binary alloys during solidi cation within additive manufacturing and casting; where we have performed large-scale, high-resolution simulations of Pu-Ga alloys. Tusas has demonstrated ideal algorithmic and parallel scaling and efficiency on up to 4 billion unknowns and over 24 thousand GPUs on the DOE leadership machines Summit and Sierra [20].

1.2 Phase field implementation within Tusas. Tusas was originally developed for phase field simulation of solidification of metals and alloys during Additive Manufacturing and casting processes. Phase field is a mathematical model for solving interfacial problems. The method substitutes boundary conditions at the interface by a partial differential equation for the evolution of the phase field or order parameter. This phase field takes two distinct values in each of the phases, with a smooth (diffuse) change between both values around the sharp interface, which is then diffuse with a finite width. It has mainly been applied to solidification dynamics.
The phase field approach depends on an appropriate physical approximation of the total free energy,

$$F(\varphi, C, T, \dots) = \int f(\varphi, C, T, \dots) + \frac{\epsilon_C^2}{2}\nabla C \cdot \nabla C + \frac{\epsilon^2}{2}\nabla\varphi \cdot \nabla\varphi + E_e(\varphi)\, d\Omega, \qquad (1)$$

where f is the free energy density (typically due to chemistry), the second term is gradient composition energy, the third term is interfacial energy density and E_e is the elastic strain density; here, φ is an order parameter (typically phase), C is concentration, and T is temperature. The free energy functional, F, describes interactions between phase(s), alloy component concentrations, temperature, stress, strain, etc. We note that the term f is generally in the form of a double well with an energy barrier of some height between the wells; and typically favors sharp interfaces between phases, while the second term favors a uniform mixture by imposing a gradient energy

penalty. Minimums of the free energy functional are obtained via variational calculus and are satisfied by:

$$\frac{\partial \varphi}{\partial t} = -M_{\varphi}\left(\frac{\partial f}{\partial \varphi} - \epsilon^2 \Delta \varphi + \frac{\partial E_e}{\partial \varphi}\right), \tag{2}$$

and

$$\frac{\partial C}{\partial t} = \nabla \cdot \left(M_C \nabla\left(\frac{\partial f}{\partial C} - \epsilon_C^2 \Delta C\right)\right). \tag{3}$$

Where (2) is the *Allen-Cahn* equation applied to non-conserved quantities and (3) is the *Cahn-Hilliard* equation applied to conserved quantities, and M_φ and M_C are mobilities; and ϵ is related to interface width. We note that (3) due to $C \neq 0$, constitutes a fourth order PDE, and is typically decoupled to two second order PDEs in practice [67]. For solidification problems typically encountered in Tusas, we have $C = 0$. For problems involving surface corrosion, we have $C \neq 0$. The evolution of the elastic energy term, E_e, is typically obtained via Newton's second law of motion [54]. Equations (2)-(3) typically constitute a large set of coupled, nonlinear, parabolic, partial differential equations at multiple time and length scales. In addition, the discretized system will be very large due to mesh resolution required to capture the di use interface.

The phase field approach for multi-component materials and alloys typically involves special treatment of the concentration fields of each component. The approach adopted in the community is that of Kim-Kim-Suzuki (KKS model) [35]. In the KKS model, the interface is treated as an equilibrium mixture of two phases with fixed compositions such that an arbitrary diffuse interface width may be specified for a given interfacial energy. For a two-component alloy, the model consists of a single order parameter and fictitious global phase concentrations C_a and C_b such that

$$C = \big(1 - h(\varphi)\big)\, C_a + h(\varphi)\, C_b, \tag{4}$$

where, $h(\varphi)$ is a smooth interpolation between phases. The free energy is decomposed as:

$$f(\varphi, C) = \big(1 - h(\varphi)\big) f_a(C_a) + h(\varphi) f_b\,(C_b), \tag{5}$$

where $f_a(C_a)$ and $f_b(C_b)$ are the phase-free energies and (5) accounts for mass conservation. The model consists of an additional constraint given by:

$$\frac{\partial f_a(C_a)}{\partial C_a} = \frac{\partial f_b(C_b)}{\partial C_b}, \tag{6}$$

which enforces pointwise equality of the phase chemical potentials. Equations (5)-(6) constitute a nonlinear algebraic system which needs to be solved at every discretization point in space. For common materials, $f_a(C_a)$ and $f_a(C_a)$ can often be obtained via a rational polynomial interpolation approach known as CALPHAD [51]. Extensions to multicomponent systems can be found in [50]. Similar treatment of the elastic energy is often required.

Our approach within Tusas is to treat (2)-(3) with unstructured finite element spatial discretization and implicit, adaptive temporal discretization to mitigate time scales and leverage hierarchical computational parallelism to mitigate length scales; and utilizes scalable and efficient algorithms, robust solvers and preconditioners, and modern computational science approaches.

We note that the phase field approach relies fundamentally on the free energy functional (1), and key experimental data or DFT data is often needed for approximation of chemical and elastic free energy. The extension of Tusas to phase field modeling of surface corrosion depends vitally upon

development of models for chemical free energy and elastic free energy within the realms of hydriding and oxidation.

2. Key knowledge gaps. We have identified key knowledge gaps for the successful extension of the Tusas phase field implementation to modeling oxidation and hydriding processes, outlined within three categories:

1. Knowledge gaps in the development of chemical free energy models
2. Knowledge gaps in the development of elastic free energy model and polycrystalline evolution
1. General requirements in transition from solidi cation models to corrosion models and capabilities for surface-environment interactions

2.1 Development of chemical free energy models: The primary knowledge gap to modeling oxidation and hydriding or surface corrosion within the phase field framework is developing suitable chemical free energy models. There has been limited experimental studies for oxidation in Pu [21, 46, 24], and more limited literature for phase field models [34]. Phase field modeling of hydride formation in metals is found more extensively in literature [30, 31, 53, 26].

In particular, continuously differentiable forms of $F_a\ (C_a)$ and $f_b(C_b)$ must be known for the materials of interest. Common forms of chemical free energy models assume temperature dependence:

$$f_{chem}(\varphi, C, T) = \big(1 - h(\varphi)\big) f_a(C_a, T) + h(\varphi) f_b(C_b, T), \qquad (7)$$

with

$$f_a(C_a, T) = A_a \left(C_a - C_a^{eq}(T)\right)^2 + B_a, \qquad (8)$$

and

$$f_b(C_b, T) = A_b \left(C_b - C_b^{eq}(T)\right)^2 + B_b, \qquad (9)$$

with $C^{eq}(T)$ obtained via experimental data or from DFT data and A, B fitting parameters. Experimental data and knowledge for development of chemical free energies for corrosion mechanisms are critical.

2.2 Development of elastic free energy model and polycrystalline evolution. Mechanical stress and strain play an important role in determining the phase transformation, thermodynamics and kinetics. Similar to chemical free energy, the elastic free energy and stress is decomposed across the phases a and b. The relationship $E_e(\varphi)$ must be known for the materials of interest, and requires development of elastic free energy in the form of (5)-(6), with $f_a(C_a)$ and $f_a(C_a)$ continuously differentiable.

Additionally, hydride/oxidation formation is associated with large volume deformation and expansion due to lower density of hydride/oxide compared to metal. To account for these deformations an additional set of PDEs for mechanical equilibrium (displacement) must be coupled to the phase field equations. Crystallographic orientation plays an important role in microstructural evolution. Prior to this project, the approach in Tusas utilized a very large number of phase field variables to describe many grains of many different orientations. This approach required an additional PDE be coupled for each orientation requiring a high computational cost.

The primary knowledge gaps for hydride an oxide modeling include development of chemical free energy; implementation of accurate elastic free energy, solution of mechanical equilibrium

equations and polycrystalline microstructure evolution model. Experimental data for these relationships is critical and not fully understood or represented with the literature presently and are critical.

2.3 Transition from solidification models to corrosion models. Common phase field models of solidification consist of evolution of species concentration in (3) with $C = 0$; while models for corrosion consist of species evolution with $C \neq 0$. Due to $C \neq 0$, (3) constitutes a fourth order PDE. The presence of $C \neq 0$ requires (3) to be decoupled to a system of two second-order PDEs, requiring an extra PDE to be solved [67, 68]. This decoupling is readily available in Tusas; however, inclusion of an additional PDE requires an additional PDE be solved at every mesh point. For high resolution simulations, this can add significant computational cost.

3. Literature review. The most detailed formulation of phase field applied to hydride formation in metals found in open literature is in a PhD thesis [31]. This work describes delta-hydride formation in alpha-Zr; including a detailed formulation of total free energy, elastic solid mechanics, and a probability-based nucleation model utilizing MOOSE and incorporates CALPHAD. A simpler presentation, though probably lacking in considerable detail can be found in [53], and a more general presentation applicable to binary metal-hydrogen systems additionally with multiply defined grains can be found in [26]. In particular, [53] provides a second order approximation to the CALPHAD system (identical to (8)-(9)) in [31]. A similar CALPHAD approach for delta-hydride and alpha-Zr can be found in [30]. A phase field model for simulating metal hydride formation involving large volume expansion in single- and polycrystals in zirconium metals. The phase field models within include diffusional and displacive phase transformations in polycrystals, inhomogeneous elasticity, solute grain boundary interaction, and structural variant-grain boundary interaction using CALPHAD via KKS. A full description of the total free energy is given. This approach utilizes a full Cahn-Hilliard for composition; FFT solution, no description of the coupling [26]. A newly developed and self-consistent CALPHAD thermodynamic database is presented which covers the elements: Pu, U, Fe, Ga across their whole composition and temperature ranges [42]. This work studies the interaction of actinides and actinide alloys such as the delta-stabilized Pu-Ga alloy with iron and is of interest to understand the impurity effects on phase stability.

General literature for hydride formation in metals include a PhD thesis on experimental formation of plutonium hydride. The central theme to this thesis is a metallographic analysis of the hydride reaction sites and the exploration of relationships between hydride and parent material microstructures. In particular, changes to the parent material surrounding the hydride reaction sites are of specific interest [8]. Closely related to previous, experimental results for formation of plutonium hydride. Experimental results show primarily the interior of the hydride reaction sites has a significantly different microstructure to that of the surrounding metal. Abstract states possible models for anisotropic growth and formation of a discontinuous interface are discussed although no clear models are presented [9]. Similar experimental results can be found in [10]. Experimental studies of kinetics in Plutonium Hydride with Oxygen can be found in [56]. An NMR study was conducted on protons in the nonstoichiometric plutonium hydride system; magnetically ordered phases at low temperatures, with experimental data was conducted in [12]. The effects of pressure and temperature upon the rate and mechanism of the reaction between plutonium and deuterium have been reported for various temperatures to and pressures [7]. Equilibrium, kinetic and X-ray diffraction data detail the existence of two stability regimes in the Pu-H system [25]. Pressure-temperature-composition data are presented for the plutonium-

hydrogen and plutonium-deuterium systems in the composition ranges Pu-PuH2 and Pu-PuD2 [43]. Pressure-Composition-Temperature (PCT) data are presented for the plutonium-hydrogen (Pu-H) and plutonium-deuterium (Pu-D) systems in the solubility region up to terminal solubility [49].

The latest edition of the Plutonium Handbook [13] provides data for Pu-H, Pu-O and Pu-Ga systems. A direct experimental comparison of variables affecting the properties of LANL-produced vs. Rocky Flats metals can be found in [65]. Reaction rates of air and oxygen with cubic plutonium hydride (PuHx,1.9<x<3), monoxide monohydride (PuOH), and Pu metal coated with these compounds are described, along with kinetic results for the Pu+H2 reaction are provided in [23]. Reference [57] provides a characterization of products formed by reacting unalloyed plutonium with water vapor. Thermodynamic properties of Pu-O system can be found in [2]; [22] provides a detailed experimental analysis of Pu-O system and oxidation processes. The reactivity of a delta-Pu alloy was studied under dry oxygen at different temperatures, with experimental results provided [48].

Resources for phase field models (2D) of delta formation in Pu-Ga are given in [29, 28]; verification data from experiments can be found in [41]. A detailed history of experimental and modeling of Pu-Ga systems is given in [40]. A suitable CALPHAD-like free energy term for Pu-Al and Pu-Ga is given in [1] (eq. 12).

Concentration-penetration data obtained with an electron microprobe analyzed and fitted by a least-squares provide an Arrhenius relationship for Pu-Ga diffusion [15]. Rafalski [47] provides an overview of experimental data for Gallium diffusion in delta-stabilized Pu-Ga alloys. Studies of self-diffusion in face-centered orthorhombic gamma phase Pu provide experimental data [58, 59, 60]. Wade [63] has determined self-diffusion coefficients for the epsilon, delta prime, delta, gamma, and beta phases of polycrystalline plutonium by the thin-film tracer technique. The self-diffusion coefficients for plutonium in a Pu 1 wt% Ga delta-stabilized alloy have been determined for various temperatures [64]; and experimental solubility measurements of H in Pu and Pu-Ga are given in [3].

Data relevant to elastic free energy and polycrystalline evolution can be found in [19]; and data for grain dislocation vacancies in Pd-H [36]. Surrogate systems for Pu-O and Pu-H can be found in [66], and an overview of methods for aged materials [52].

4 Tusas code enhancements. We have made the following code enhancements to Tusas over the course of the project:

4.1 Polycrystalline evolution model enhancements. Hydriding and oxidation evolution requires extension of our elastic free energy model and polycrystalline evolution model, as mechanical stress and strain play a critical role in determining the phase transformation thermodynamics and kinetics. Elastic free energy additionally requires solution of the mechanical equilibrium equations with crystallographic orientation, represented by quaternions. In support of hydriding and oxidation evolution, we have implemented local manifold projection temporal integration to support quaternion evolution. This approach provides an alternative to using a very large number of phase field variables to describe many grains of many different orientations. The quaternion describes the local grain orientation within a crystal. This approach introduces a vector

$$\mathrm{q} = [q_1\ q_2\ q_3\ q_4]^{\mathrm{T}},$$

that evolves as a solution to a partial differential equation and the constraint [17]:

$$\sum_{i=1}^{4} q_i^2 = 1.$$

The constraint constitutes a projection onto a local manifold; performed at the end of the corrector step in the adaptive temporal integration. This capability has been verified and is implemented within a Tusas regression test with

$$\mathrm{q} = [q_1\ q_2]^{\mathrm{T}}.$$

Figure 1 shows results the computed solution; the exact analytic solution; and norm of the computed solution from our Tusas regression test problem. Figure 2 shows the temporal error for each component. Full quaternion support is being tested.

Similar to chemical free energy, the elastic free energy and stress is decomposed across phases; where φ assumes a role of structural order parameter. Elastic modulus and eigenstrain are assumed as functions structural order parameter only, and the elastic free energy additionally requires solution of the mechanical equilibrium equations. Experimental data for development of elastic free energies for corrosion mechanisms are critical; in particular mechanical properties derived from experimental data is critical for adaption of our existing models to corrosion.

4.2 Surface energy deposition enhancements. In support of surface energy and environment interactions, we have implemented 3D radiative and convective (nonlinear) Neumann boundary conditions within the Tusas code [27, 14, 44]. The verification model consists of a 3D domain consisting of a ceramic strip that is embedded in a high-thermal-conductive material. The side boundaries of the strip are maintained at a constant temperature (Dirichlet boundary condition). The top surface of the strip is losing heat via both thermal convection and thermal convection to the ambient environment. The bottom boundary, however, is assumed to be thermally insulated (homogeneous Neumann boundary condition). Simulation results have been verified against the literature and implemented within the Tusas regression testsuite and shown in Figure 3.

4.3 Adaptive time integration enhancements. The polycrystalline evolution and surface energy deposition simulation results were obtained utilizing second order adaptive time integration with an Adams-Bashforth predictor and Trapezoid Rule corrector method (AB-TR). The ABTR method is a substantial improvement over the existing first order forward Euler predictor and backward Euler corrector method (FE-BE) implemented in previously in Tusas. Preliminary results show a speedup of 13x for AB-TR over **fi**xed timestep TR for a given level of accuracy for this simulation. Figure 4 shows cost in terms of CPU for time integration to t=.0001 for AB-TR with adaptive time steps and TR with fixed time step size. AB-TR requires 55.95seconds and TR requires 764 seconds for time integration to t=.0001. In this case, for a given level of accuracy, AB-TR requires 0.08% of the computational resources than TR.

4.4 Autocatalytic chemical reactions in Tusas. We have added direct support for autocatalytic chemical reactions in Tusas. A single chemical reaction is said to be autocatalytic if one of the reaction products is also a catalyst for the same or a coupled reaction [37, 11, 55, 39, 38, 4]. Such a reaction is called an autocatalytic reaction. Support for time-dependent chemical reactions in Tusas configurable at runtime, with a runtime interface for reaction rates and initial conditions. Third order autocatalytic reaction (second-order adaptive timestep) added to the Tusas regression testing suite:

$$A \overset{k_1}{\rightarrow} B + C$$

$$A + B \xrightarrow{k_2} A\,B$$

$$A\,B \xrightarrow{k_3} 2B + C.$$

Results have been verified against the literature and shown in Figure 5. This capability is a critical tool for estimation of reaction rates within experiments.

5. References.

[1] PH Adler. Thermodynamic equilibrium in the low-solute regions of Pu-group MIA metal binary systems. Metallurgical Transactions A,22(10):2237-2246, 1991.

[2] VV Akhachinkii. IAEA symposium on thermodynamics of nuclear materials, 1963.

[3] TH Allen. The Solubility of Hydrogen in Plutonium in the Temperature Range 475 to 826 Degrees Centigrade. PhD thesis, Thesis, University of Colorado at Denver, Denver, CO, 1991.

[4] Erdem Arslan and Ian J Laurenzi. Kinetics of autocatalysis in small systems. The Journal of chemical physics, 128(1):01B602, 2008.

[6] C Beckermann, H-J Diepers, I Steinbach, A Karma, and X Tong. Modeling melt convection in phase-field simulations of solidifiation. Journal of Computational Physics, 154(2):468-496, 1999.

[7] David F Bowersox. Reaction between plutonium and deuterium. part ii. rate measurements by weight changes. Technical report, Los Alamos Scientific Lab., NM (USA), 1977.

[8] Martin Brierley. Microstructural and morphological aspects of plutonium hydride. PhD thesis, University of Manchester, 2016.

[9] Martin Brierley, John Philip Knowles, Andrew Sherry, and Michael Preuss. The anisotropic growth morphology and microstructure of plutonium hydride reaction sites. Journal of Nuclear Materials, 469:145-152, 2016.

[10] Martin Brierley, John Philip Knowles, Andrew Sherry, and Michael Preuss. The anisotropic growth morphology and microstructure of plutonium hydride reaction sites. Journal of Nuclear Materials, 469:145-152, 2016.

[11] C. Capellos and B.H.J. Bielski. Kinetic Systems: Mathematical Description of Chemical Kinetics in Solution. Wiley-Interscience, 1972.

[12] G Cinader, D Zamir, and Z Hadari. Nmr study of the plutonium hydride system. Physical Review B, 14(3):912, 1976.

[13] David L Clark, David A Geeson, and Robert J Hanrahan. Plutonium handbook, volume 6. American Nuclear Society La Grange Park, Illinois, USA, 2019.

[14] John Coleman, Alex Plotkowski, Benjamin Stump, Narendran Raghavan, AS Sabau, MJM Krane, Jarred Heigel, RE Ricker, Lyle Levine, and SS Babu. Sensitivity of thermal predictions to uncertain surface tension data in laser additive manufacturing. Journal of Heat Transfer, 142(12),

2020.

[15] GR Edwards, RE Tate, and EA Hakkila. Di usion in stabilized delta plutonium, i. gallium. Journal of Nuclear Materials, 25(3):304-309, 1968.

[16] J-L Fattebert, ME Wickett, and PEA Turchi. Phase-field modeling of coring during solidification of Au-Ni alloy using quaternions and calphad input. Acta materialia, 62:89-104, 2014.

[17] J-L Fattebert, ME Wickett, and PEA Turchi. Phase-field modeling of coring during solidification of Au-Ni alloy using quaternions and calphad input. Acta materialia, 62:89-104, 2014.

[18] Marianne M Francois, Amy Sun, Wayne E King, Neil Jon Henson, Damien Tourret, Curt Allan Bronkhorst, Neil N Carlson, Christopher Kyle Newman, T Haut, Jozsef Bakosi, et al. Modeling of additive manufacturing processes for metals: Challenges and opportunities. Current Opinion in Solid State and Materials Science, 21(4):198-206, 2017.

[19] Yuh Fukai. Formation of superabundant vacancies in m-h alloys and some of its consequences: a review. Journal of Alloys and Compounds, 356:263-269, 2003.

[20] Supriyo Ghosh, Christopher K Newman, and Marianne M Francois. Tusas: A fully implicit parallel approach for coupled phase-field equations. Journal of Computational Physics, 448:110734, 2022.

[21] Petronela Gotcu-Freis. High temperature thermodynamic studies on the transuranium oxides and their solid solutions. Ios Press, 2011.

[22] JM Haschke, Thomas H Allen, and Luis A Morales. Surface and corrosion chemistry of plutonium. Los Alamos Sci, 26(2):252-273, 2000.

[23] John M Haschke and Thomas H Allen. Plutonium hydride, sesquioxide and monoxide monohydride: pyrophoricity and catalysis of plutonium corrosion. Journal of alloys and compounds, 320(1):58-71, 2001.

[24] John M Haschke, Thomas H Allen, and Luis A Morales. Reaction of plutonium dioxide with water: formation and properties of puo2+ x. science, 287(5451):285-287, 2000.

[25] John M Haschke, Angelo E Hodges III, C Michael Smith, and Franklin L Oetting. Equilibria and thermodynamic properties of the plutonium hydrogen system. Journal of the Less Common Metals, 73(1):41-48, 1980.

[26] Tae Wook Heo, Kimberly B Colas, Arthur T Motta, and Long-Qing Chen. A phase-field model for hydride formation in polycrystalline metals: Application to delta-hydride in zirconium alloys. Acta Materialia, 181:262-277,2019.

[27] Jack Philip Holman. Heat Transfer. Tata McGraw-Hill Education, 2008.

[28] S. Y. Hu, M. I. Baskes, M. Stan, J. N. Mitchell, J. X. Zhang, and L. Q. Chen. Effect of Elastic Anisotropy and Inhomogeneity on Coring Structure Evolution in Pu-Ga Alloys Phase- eld modeling. Journal of Computer-Aided Materials Design, 14(3):389-402, October 2007.

[29] SY Hu, M Baskes, M Stan, and J Mitchell. Phase-field modeling of coring structure evolution in pu-ga alloys. Acta materialia, 55(11):3641-3648, 2007.

[30] A.M. Jokisaari and K. Thornton. General method for incorporating calphad free energies of mixing into phase eld models: Application to the alpha-zirconium/ delta-hydride system. Calphad, 51:334-343, 2015.

[31] Andrea M Jokisaari. Multiphysics Phase Field Modeling of Hydrogen Diffusion and delta-Hydride Precipitation in alpha-Zirconium. PhD thesis, 2016.

[32] Alain Karma and Wouter-Jan Rappel. Phase-field method for computationally efficient modeling of solidification with arbitrary interface kinetics. Phys. Rev. E, 53(4):R3017-R3020, 1996.

[33] Alain Karma and Wouter-Jan Rappel. Quantitative phase-field modeling of dendritic growth in two and three dimensions. Phys. Rev. E, 57(4):4323-4349, 1998.

[34] Kyoungdoc Kim, Quentin C Sherman, Larry K Aagesen, and Peter W Voorhees. Phase-field model of oxidation: Kinetics. Physical Review E, 101(2):022802, 2020.

[35] Seong Gyoon Kim, Won Tae Kim, and Toshio Suzuki. Phase-field model for binary alloys. Phys. Rev. E, 60:7186-7197, Dec 1999.

[36] Reiner Kirchheim. Reducing grain boundary, dislocation line and vacancy formation energies by solute segregation. i. theoretical background. Acta Materialia, 55(15):5129-5138, 2007.

[37] Yury Kryvasheyeu. The phase field simulation of autocatalytic nucleation. PhD thesis, Monash University, 2012.

[38] D Lavabre, V Pimienta, G Levy, and JC Micheau. Reversible, mixed first- and second-order and autocatalytic reactions as particular cases of a single kinetic rate law. The Journal of Physical Chemistry, 97(20):5321-5326, 1993.

[39] TR Marchant. Cubic autocatalytic reaction-diffusion equations: semi-analytical solutions. Proceedings of the Royal Society of London. Series A: Mathematical, Physical and Engineering Sciences, 458(2020):873-888, 2002.

[40] Jeremy N Mitchell, Daniel S Schwartz, Marius Stan, and Carl J Boehlert. Phase stability and phase transformations in plutonium and plutonium-gallium alloys. Metallurgical and Materials Transactions A, 35(8):2267-2278, 2004.

[41] JN Mitchell, FJ Freibert, DS Schwartz, and ME Bange. Unconventional delta-phase stabilization in pu-ga alloys. Journal of nuclear materials, 385(1):95-98, 2009.

[42] Emily E Moore, Patrice EA Turchi, Alexander Landa, Per Sooderlind, Benoit Oudot, Jonathan L Belof, Stephen A Stout, and Aurelien Perron. Development of a calphad thermodynamic database for pu-u-fe-ga alloys. Applied Sciences, 9(23):5040, 2019.

[43] Robert NR Mulford and Gladys E Sturdy. The plutonium-hydrogen system.i. plutonium dihydride and dideuteride1. Journal of the American Chemical Society, 77(13):3449-3452, 1955.

[44] Saralees Nadarajah. A generalized normal distribution. Journal of Applied statistics, 32(7):685-694, 2005.

[45] Christopher K. Newman. Tusas. https://github.com/chrisknewman/tusas, 2022.

[46] Ruizhi Qiu, Xin Wang, Yongbin Zhang, Bingyun Ao, and Kezhao Liu. Thermodynamical stability of plutonium monoxide with carbon substitution. The Journal of Physical Chemistry C, 122(40):22821-22828, 2018.

[47] AL Rafalski, MR Harvey, and DH Riefenberg. Gallium diffusion in delta-stabilized Pu-ga alloys. Technical report, Dow Chemical Co., Golden, Colo., 1967.

[48] B Ravat, L Jolly, B Oudot, A Fabas, H Guerault, I Popa, and F Delaunay. New insight into delta-pu alloy oxidation kinetics highlighted by using in-situ x-ray diffraction coupled with an original rietveld refinement method. Corrosion Science, 138:66-74, 2018.

[49] Scott Richmond, Jon S Bridgewater, John W Ward, and Thomas H Allen. The solubility of hydrogen and deuterium in alloyed, unalloyed and impure plutonium metal. In IOP Conference Series: Materials Science and Engineering, volume 9, page 012036. IOP Publishing, 2010.

[50] Boina Sagar, Krishanu Biswas, and Rajdip Mukherjee. A phase-field study on a eutectic high-

entropy alloy during solidification. Philosophical Magazine Letters, 101(4):160-172, 2021.

[51] Nigel Saunders and A Peter Miodownik. CALPHAD (calculation of phase diagrams): a comprehensive guide. Elsevier, 1998.

[52] AJ Schwartz and WG Wolfer. Overview of modeling and simulations of plutonium aging. Journal of Computer-Aided Materials Design, vol. 14, no. 3, September 30, 2007, pp. 331-335, 14(UCRL-JRNL-230302), 2007.

[53] Wooseob Shin and Kunok Chang. Phase-field modeling of hydride reorientation in zirconium cladding materials under applied stress. Computational Materials Science, 182:109775, 2020.

[54] W.S. Slaughter. The Linearized Theory of Elasticity. Birkhhauser Boston, 2002.

[55] George D Snell. An inherent defect in the theory that growth rate is controlled by an autocatalytic process. Proceedings of the National Academy of Sciences of the United States of America, 15(3):274, 1929.

[56] Jerry L Stakebake. Kinetic studies of the reaction of plutonium hydride with oxygen. Nuclear Science and Engineering, 78(4):386-392, 1981.

[57] Jerry L Stakebake, DT Larson, and John M Haschke. Characterization of the plutonium-water reaction ii: formation of a binary oxide containing pu (vi). Journal of alloys and compounds, 202(1-2):251-263, 1993.

[58] RE Tate, EM Cramer, and AS Goldman. Self-diffusion studies of delta plutonium. appendix least-squares technique for estimating diffusion parameters. Trans. AIME, 230, 1964.

[59] RE Tate and GR Edwards. Self-diffusion studies of gamma plutonium. Technical report, Los Alamos Scientific Lab., Univ. of California, N. Mex., 1964.

[60] RE Tate and GR Edwards. Self-diffusion studies of gamma-plutonium; etude de l'autodi usion du plutonium gamma; izuchenie gamma-plutoniya sposobom samodi uzii; estudios de autodifusion del plutonio gamma. 1966.

[61] Amelia J. Trainer, Christopher Kyle Newman, and Marianne M. Francois. Overview of the tusas code for simulation of dendritic solidification. Los Alamos National Lab. (LANL), Los Alamos, NM (United States) LA-UR-16-20078

[62] John A Turner, James Belak, Nathan Barton, Matthew Bement, Neil Carlson, Robert Carson, Stephen DeWitt, Jean-Luc Fattebert, Neil Hodge, Zechariah Jibben, et al. Exaam: Metal additive manufacturing simulation at the fidelity of the microstructure. The International Journal of High Performance Computing Applications, 36(1):13--39, 2022.

[63] Warren Z Wade, David W Short, John C Walden, and Joseph W Magana. Self-diffusion in plutonium metal. Metallurgical Transactions A, 9(7):965-972, 1978.

[64] WZ Wade. The self-di usion of plutonium in a pu/1 wt% ga alloy. Journal of Nuclear Materials, 38(3):292-302, 1971.

[65] John W Ward, Scott Richmond, and Franz J Freibert. Comparison of variables affecting the properties of lanl-produced vs. rocky flats metals (u). Technical report, Los Alamos National Lab.(LANL), Los Alamos, NM (United States), 2011.

[66] DW Wheeler, Jurgita Zekonyte, and RJK Wood. Structure and mechanical properties of ce-la alloys containing 3-10 wt.% la. Journal of Nuclear Materials, 543:152497, 2021.

[67] Qiongwei Ye, Zhigang Ouyang, Chuanjun Chen, and Xiaofeng Yang. Efficient decoupled

second-order numerical scheme for the flow-coupled cahn-hilliard phase-field model of two-phase flows. Journal of Computational and Applied Mathematics, 405:113875, 2022.

[68] Liangzhe Zhang, Michael R Tonks, Derek Gaston, John W Peterson, David Andrs, Paul C Millett, and Bulent S Biner. A quantitative comparison between c0 and c1 elements for solving the cahn-hilliard equation. Journal of Computational Physics, 236:74-80, 2013.

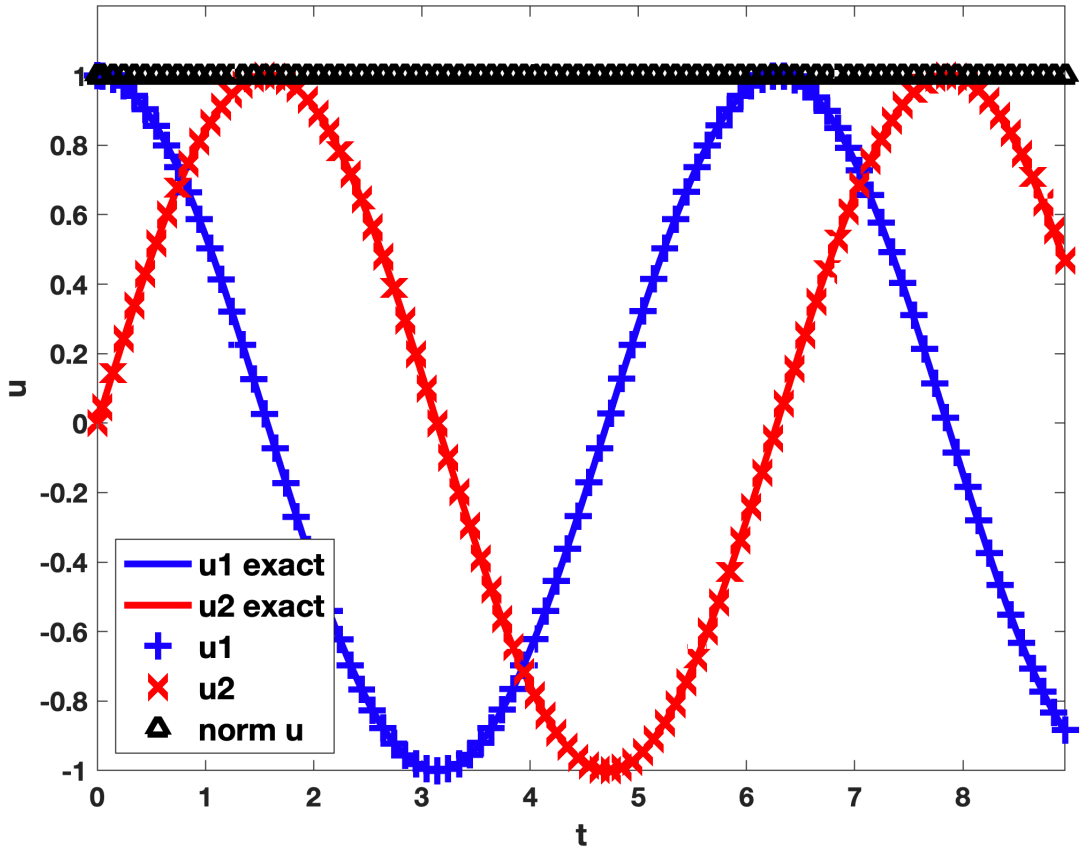

Figure 1: Quaternion implementation in Tusas test suite.

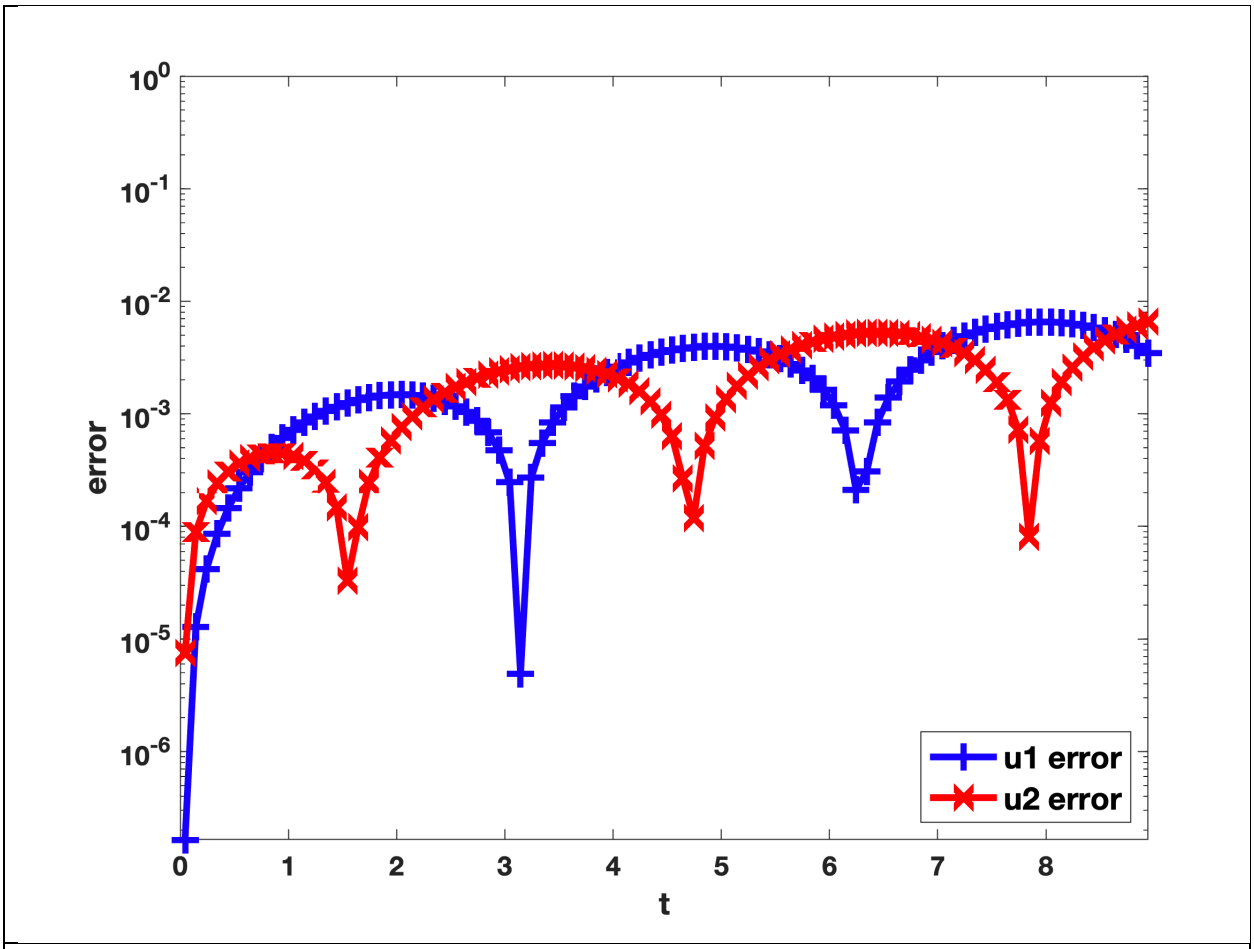

Figure 2: Quaternion error.

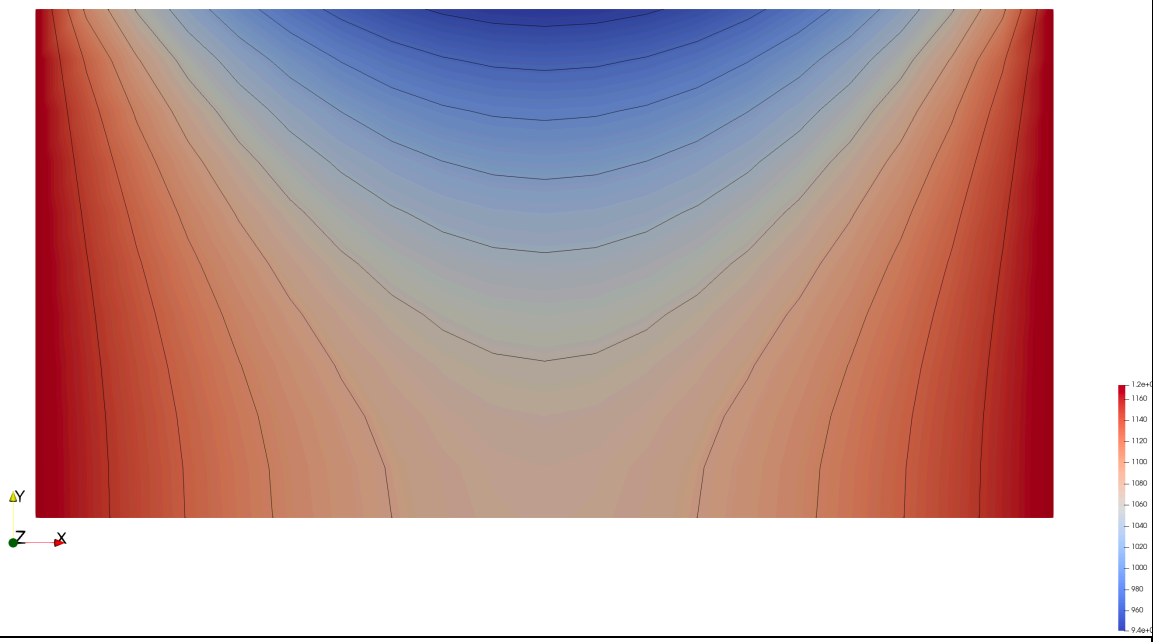

Figure 3: Surface energy deposition implementation in Tusas test suite.

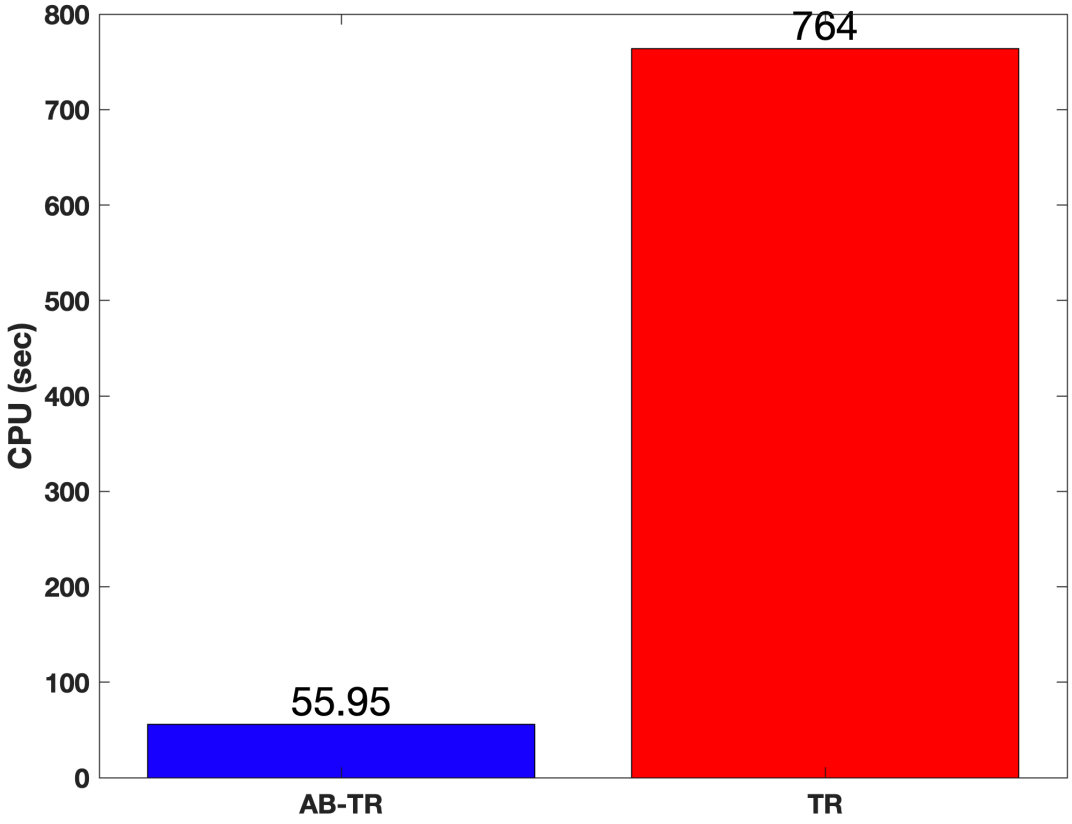

Figure 4: Cost in terms of CPU for time integration to t=.0001 for AB-TR with adaptive time steps and TR with fixed time step size.

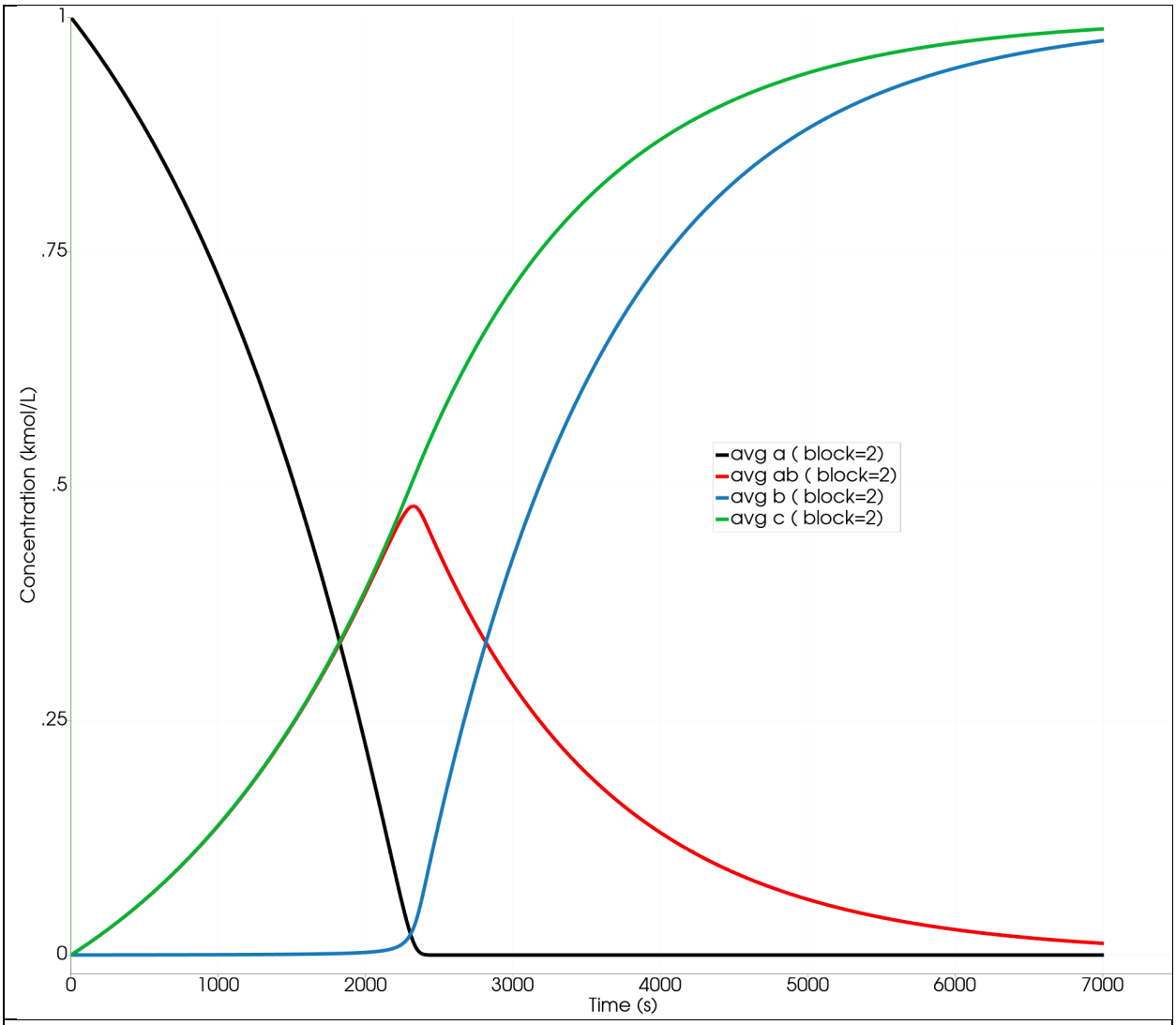

Figure 5: Autocatalytic implementation in Tusas test suite.